

DOE/ER/05023--3
CONF-8406182--2

NEUTRAL-CURRENT x-DISTRIBUTIONS

D.Bogert, R.Burnstein, R.Fisk, S.Fuess, J.Morfin,
T.Ohska, L.Stutte, J.K.Walker
Fermi National Accelerator Laboratory
Batavia, Illinois 60510, USA

J.Bofill, W.Busza, T.Eldridge, J.I.Friedman, M.C.Goodman,
H.W.Kendall, I.G.Kostoulas, T.Lyons, R.Magahiz, T.Mattison,
A.Mukherjee, L.S.Osborne, R.Pitt, L.Rosenson, A.Sandacz,
M.Tartaglia, F.E.Taylor, R.Verdier, S.Whitaker, G.P.Yeh
Massachusetts Institute of Technology
Cambridge, Massachusetts 02139, USA

M.Abolins, R.Brock, A.Cohen, J.Ernwein, D.Owen, J.Slate, H.Weerts
Michigan State University
East Lansing, Michigan 48824, USA

(presented by S.Fuess)
June 1984

ABSTRACT

The role of the semi-leptonic neutral current interaction as a probe of nucleon structure is examined. Previous measurements of neutral current x-distributions are reviewed, and new results from the Fermilab - MIT - MSU collaboration are presented.

MASTER

1. Introduction

The studies of deep inelastic electron, muon, and charged current (CC) neutrino scattering have revealed much about the structure of the nucleon. Subtle differences are expected to exist between the nucleon structure functions as determined by the two weak gauge boson probes, W^+ and Z^0 . The charged current interaction must transform the charge of the struck quark, whereas the neutral current interaction is believed to be a flavor "diagonal" interaction and therefore does not couple different quark flavors. In addition, there could be an as yet unobserved quark structure which interacts preferentially with the weak neutral current. It is natural therefore to ask whether the analysis of deep inelastic neutral current (NC) neutrino scattering data confirms our present understanding of the structure of the nucleon.

The differential cross-section for neutrino deep inelastic scattering is given by:

$$(d^2\sigma)/(dx dy) = G^2 M E_\nu / \pi [(1-y+y^2/2) F_2(x) + (y-y^2/2) x F_3(x)] \quad (1)$$

NOTICE

PORTIONS OF THIS REPORT ARE ILLEGIBLE.

It has been reproduced from the best available copy to permit the broadest possible availability.

DISTRIBUTION OF THIS DOCUMENT IS UNLIMITED

zhp

PUBLICLY RELEASABLE
L. C. McNamee
Authorizing Official
Date: 05/01/2006

DISCLAIMER

This report was prepared as an account of work sponsored by an agency of the United States Government. Neither the United States Government nor any agency Thereof, nor any of their employees, makes any warranty, express or implied, or assumes any legal liability or responsibility for the accuracy, completeness, or usefulness of any information, apparatus, product, or process disclosed, or represents that its use would not infringe privately owned rights. Reference herein to any specific commercial product, process, or service by trade name, trademark, manufacturer, or otherwise does not necessarily constitute or imply its endorsement, recommendation, or favoring by the United States Government or any agency thereof. The views and opinions of authors expressed herein do not necessarily state or reflect those of the United States Government or any agency thereof.

DISCLAIMER

Portions of this document may be illegible in electronic image products. Images are produced from the best available original document.

where the $(-)+$ is for (anti)neutrino scattering. Equation (1) makes the normal assumptions of scaling and the validity of the Callan-Gross relation, $2xF_1(x)=F_2(x)$. The x -dependence of the cross-section is often written in terms of the structure functions $F_{\pm}(x)$ as:

$$d\sigma/dx = G^2ME_{\nu} / (2\pi) F_{\pm}(x) \quad (2)$$

where again the $(-)+$ is for (anti)neutrino scattering. The structure functions $F_{\pm}(x)$ are combinations of the structure functions $F_2(x)$ and $xF_3(x)$.

In the context of the quark-parton model the structure functions are related to the momentum fraction distributions of the quarks in the nucleon. The CC structure functions are:

$$\begin{aligned} F_2(x) &= xq(x) + x\bar{q}(x) \\ xF_3(x) &= xq(x) - x\bar{q}(x) \pm 2[xs(x)-xc(x)] \end{aligned} \quad (3)$$

where the $(-)+$ is for (anti)neutrino scattering, and where:

$$\begin{aligned} q(x) &= u(x) + d(x) + s(x) + c(x) \\ \bar{q}(x) &= \bar{u}(x) + \bar{d}(x) + \bar{s}(x) + \bar{c}(x) \end{aligned} \quad (4)$$

and where a symmetrical sea-quark distribution is assumed:

$$q(x)_{\text{sea}} = \bar{q}(x)_{\text{sea}} \quad (5)$$

The NC structure functions have different contributions from the strange and charm sea in addition to being modified by the quark coupling constants:

$$\begin{aligned} F_2(x) &= (u_L^2+d_L^2+u_R^2+d_R^2)[xq(x)+x\bar{q}(x)] \\ &\quad - (u_L^2-d_L^2+u_R^2-d_R^2)2[xs(x)-xc(x)] \\ xF_3(x) &= (u_L^2+d_L^2-u_R^2-d_R^2)[xq(x)-x\bar{q}(x)] \end{aligned} \quad (6)$$

Neutral current experiments can observe only the recoil hadron shower from a neutrino interaction, and not the scattered lepton. Complete kinematic reconstruction of an event requires knowledge of the recoil shower energy and angle in addition to knowledge of the energy of the incident neutrino. Reconstruction of both the shower energy and angle is presently possible only in bubble chambers or fine-grained electronic calorimeters. The incident neutrino energy is estimated using the properties of a narrow-band neutrino beam.

The scaling variable x is computed from the incident neutrino energy (E_{ν}), the recoil hadron shower energy (E_H) and angle (θ_H), and the nucleon mass (M) as:

$$x = \frac{E_\nu(E_H - M)\sin^2\theta_H}{2M[E_\nu\cos^2\theta_H - (E_H - M)]} \quad (7)$$

The ambiguity of the neutrino parent in a narrow-band beam leads to an ambiguity in the neutrino energy. The momentum spread and divergence of the secondary beam, as well as the uncertainty in the secondary decay point, also contribute to an uncertainty in the incident neutrino energy. An experiment's ability to measure the NC x-distribution depends upon the detector's resolution of hadron energy and critically upon its resolution of the hadron shower angle.

2. Columbia - Rutgers - Stevens Collaboration

The first experiment to publish results on NC x-distributions at low neutrino energies was performed by the Columbia - Rutgers - Stevens collaboration using the BNL 7-ft bubble chamber.^{1]} The experiment was performed in a narrow-band beam with positively charged secondaries of momentum 10 GeV/c. CC events were identified by at least one negative track leaving the chamber; other events were classified as NC. To reduce contamination from cosmic-ray and neutral hadron interactions, the NC sample has additional restrictions on the angle and invariant mass of the hadron shower.

After all cuts, 23 NC events remain. The x-distribution for the NC events is shown in Figure 1(a), and can be compared to the x-distribution of the CC events in Figure 1(b). The NC distribution has been corrected for cuts and resolution. While the NC and CC x-distributions are similar, the small number of events prevents any quantitative comparison.

3. CHARM Collaboration

The CHARM collaboration was the first to report results on NC x-distributions at high energies using a massive electronic calorimeter.^{2]} The CHARM fine-grained detector was exposed to the CERN 200 GeV/c narrow-band beam with both neutrinos and antineutrinos. Due to the inherent beam momentum spread and ambiguity between neutrinos from pion and kaon decay, and limitations of experimental resolutions, particularly in the hadron shower angle, an event-by-event kinematic reconstruction was not possible. Instead, the distributions in the measured variables were unfolded to determine the x-distribution. The unfolding method was applied similarly to CC events to determine its validity.

The aim was to obtain the x-distributions $F_\pm(x)$. The event distribution in the observed variables was represented as a convolution of $F_\pm(x)$ with a function which included the beam flux, the y-dependence[±], and resolutions. The unfolding consisted of

determining the $F_{\pm}(x)$ which yielded the best fit to the measured event distributions.

Events induced by neutrinos from both pion and kaon decay were used, with corrections for their relative contributions included in the unfolding procedure. Also included were corrections for beam background: either neutrinos produced before momentum selection (wide-band background) or electron neutrinos produced by K_{e3} decays. The misidentification of NC and CC events was also corrected in the unfolding procedure. Table 1 summarizes the event samples and the estimated magnitude of the background corrections.

Table 1
CHARM Event numbers and backgrounds

	ν		$\bar{\nu}$	
	NC	CC	NC	CC
raw events	2352	6496	1021	2689
K_{e3}	-191	-	-42	-
WBB	-60	-81	-92	-197
CC \leftrightarrow NC	-134	+134	-24	+24
corrected events	1967	6549	863	2516

The unfolded x-distributions $F_{\pm}(x)$ for CC and NC interactions are shown in Figure 2. The \pm points represent the unfolded x-distributions, with the plotted errors corresponding to the diagonal elements of the covariance matrix. The solid curves correspond to structure function fits of Table 2, and the histograms show the results of a CC analysis using the muon measurement. The agreement of the unfolded CC distribution with that obtained from the standard analysis demonstrates the reliability of the technique.

A quantitative comparison of the NC and CC x-distributions was made by fitting a parameterization of the valence and sea quark distribution functions:

$$\begin{aligned} q_{val}(x) &= [3/\beta(a,b+1)] x^a (1-x)^b \\ q_{sea}(x) &= C (c+1) (1-x)^c \end{aligned} \quad (8)$$

where $\beta(a,b+1)$ is the Euler beta function used to provide the normalization $\int (q_{val}/x) dx = 3$ predicted by the Gross - Llewellyn Smith sum rule. The parameter C is the integral over the sea-quark content of the nucleon, and was used to calculate the relative antiquark content $\bar{q}/(q+\bar{q})$. The shape of the sea-quark distribution was fixed by setting the parameter $c=6.18$. The remaining parameters were found by simultaneous fits to neutrino and antineutrino data. The results for

the standard CC analysis and for the unfolding analyses of CC and NC are shown in Table 2. The agreement of the CC analyses again verifies the unfolding technique. The agreement of the CC and NC parameters indicates that there is no significant difference in nucleon structure as found in CC or NC reactions.

Table 2
CHARM Fit results

Parameter	CC with muon measurement	CC from unfolding	NC from unfolding	Systematic errors
a	0.47±0.02	0.45±0.05	0.44±0.05	±0.05
b	2.71±0.11	2.97±0.16	2.79±0.24	±0.09
$\bar{q}/(q+\bar{q})$	0.14±0.005	0.17±0.03	0.13±0.03	±0.02

4. Columbia - Rutgers - BNL Collaboration

The results of a bubble chamber study of high energy NC interactions have recently been published by a Columbia - Rutgers - BNL collaboration.^{3]} The Fermilab 15-ft bubble chamber was exposed to a narrow-band neutrino beam with selected secondary momenta of 125, 140, 165, 200, and 250 GeV/c. An important feature of the analysis was the event-by-event kinematic reconstruction using the measured hadronic shower properties and the energy - radius correlation of the narrow-band beam.

The hadronic energy was corrected for the contribution of undetected neutrals. The correction was 11% for hadronic energy less than 20 GeV, and rose linearly to 35% at 100 GeV. The correction for NC events being incorrectly identified as CC events because of pion punchthrough was (8±3)%. An identified neutral hadron background subtraction of 57 events was made from the 208 NC candidates. The residual correction for unidentified neutral hadron interactions was (15±3)% of the NC sample.

The incident neutrino energy was calculated to about 10% using the energy - radius correlation of the narrow-band beam, but was ambiguous between the two values predicted for pion or kaon decay. To resolve this ambiguity, the neutrino parentage was assigned on the basis of the measured hadronic energy; if the hadronic energy was smaller (greater) than 1.1 times the predicted neutrino energy assuming the pion decay hypothesis, then events were assigned the pion (kaon) decay hypothesis. Analysis of CC events including the muon information showed this assignment to be correct at the 90% level.

The final sample of events consisted of 151 NC and 683 CC

interactions. The distributions of the scaling variable x are shown in Figure 3. The distributions are corrected for the effects of the background corrections, the cuts, and the misallocation of events between the pion and kaon decay hypotheses.

The CC distribution makes use of the information from the outgoing muon. The NC distribution is corrected for the effects of reconstructing the outgoing neutrino. The correction was made by comparing the reconstructed outgoing lepton in the CC events to the measured muon. Both distributions are also corrected for track measurement resolutions. The resolution in x after both corrections is $\sigma_x \approx 0.09$.

The structure function $F_2^+(x)$ was obtained using the observed NC to CC cross-section ratio of 0.29 ± 0.04 and the previously measured CC total cross section of $\sigma/E_\nu = (0.62 \pm 0.05) \cdot 10^{-38} \text{ cm}^2/\text{GeV}$. The distributions of $F_2^+(x)$ are shown in Figure 4. The shapes of the NC and CC distributions are observed to be consistent with each other.

5. Fermilab - M.I.T. - M.S.U. Collaboration

The fine-grained calorimeter of the Fermilab - M.I.T. - M.S.U. collaboration recently was exposed to the narrow-band beam at Fermilab. The detector consists of a calorimeter with 608 flash chamber planes in three views and 37 proportional tube planes, and a muon spectrometer of iron toroids and proportional tube planes. Figure 5 shows a CC event in the detector, demonstrating the fine granularity of the sampling of the shower development. The resolution of the reconstructed angle of the hadron shower has been measured in a hadron test beam to be $\sigma(\theta_H)_{\text{proj}} = 0.007 + 1.008/E_H(\text{GeV})$ radians.

The analysis goal was an event-by-event measurement of the scaling variable x for both NC and CC events by using the information from the hadron shower and the neutrino energy - radius correlation of the narrow-band beam. To achieve this goal, a kinematic regime was selected to enhance NC identification and kinematic reconstruction. NC and CC events were analyzed identically; the information from the muon was used only to identify CC and as checks in the kinematic reconstruction. We have also examined the ratio

$$R(x) = \frac{(\frac{d\sigma}{dx})_{\text{NC}}}{(\frac{d\sigma}{dx})_{\text{CC}}} \quad (9)$$

as a means of reducing sensitivity to systematic errors.

The narrow-band beam was set for neutrino production at three different secondary momentum selections (+165, +200, +250 GeV/c) and for antineutrino production at one selection (-165 GeV/c). Data from

each secondary momentum selection were analyzed independently to demonstrate the variations of backgrounds and the consistency of results. The final fits to the quark distribution parameters were performed simultaneously to the complete data set.

The cuts on the data are motivated by the goal of accurate event identification and reconstruction. The first cut on the data was a requirement of 10 GeV in visible hadron energy. This cut is conservatively above the trigger energy threshold for both NC and CC events. The next requirement is that the scaling variable y be less than 0.8, where y is computed from the measured hadron energy and the neutrino energy (found using the energy - radius correlation assuming pion decay) as $y = E_H / E_\nu$. This cut strongly enhances the separation of NC and CC events, as can be seen by the slight remaining misclassification of events indicated in Table 3.

Table 3
Fermilab-MIT-MSU NC - CC classification efficiencies

ν	Identified as:		
		NC	CC
Actual:	NC	.98	.02
	CC	.02	.98
$\bar{\nu}$	Identified as:		
		NC	CC
Actual:	NC	.98	.02
	CC	.01	.99

For the CC interaction the ambiguity between incident neutrinos from pion decay and those from kaon decay can be largely resolved by examination of the total (hadron plus muon) visible energy of the event. For NC interactions the identification of the neutrino parent must be accomplished with only the information from the hadronic shower and the event vertex radial position. To enhance the probability of the correct identification of the neutrino parent, we have chosen to examine the region dominated by neutrinos from pion decay. We thus require the vertex of the event to be within 1.0 meter of the beam center and require the hadron shower energy to be less than the mean energy of a pion-parent neutrino at the measured radial position. Table 4 lists the remaining contaminations of neutrinos from sources other than pion decay. The reconstruction of the event kinematics then proceeds with the pion decay hypothesis.

Table 4
Fermilab-MIT-MSU Neutrino decay parents

Decay	Secondary momentum			
	+165	+200	+250	-165
$\pi \mu 2$.893	.858	.808	.917
$K \mu 2$.083	.102	.135	.063
$K \mu 3$.003	.005	.006	.002
$K e 3$.014	.028	.041	.014
$W B B$.007	.007	.010	.003

Table 5 gives the number of events after all cuts. Kinematic reconstruction is identical for both NC and CC events. The distributions of the measured scaling variable x are shown in Figure 6 for each of the beam secondary momenta. The data points and the vertical axis scales are for the NC events. The histograms show the CC distributions, normalized to equal number of events. The x -distributions are corrected only for the effects of misclassification between NC and CC event types. Radiative corrections to the CC distributions have not been made, but are expected to be small. The NC and CC x -distributions are seen to be in excellent qualitative agreement. The ratios of the measured x -distributions, $R(x)$, are plotted in Figure 7 for each of the beam secondary momenta.

Table 5
Fermilab-MIT-MSU Final event numbers

Secondary Momentum	NC	CC
+165	873	2766
+200	590	1992
+250	548	1784
-165	597	1563

A quantitative analysis of the ratio $R(x)$ can be made by parameterizing the structure functions $\tilde{F}_2(x)$ and $x\tilde{F}_3(x)$ as

$$\begin{aligned} \tilde{F}_2(x) &= xq(x) + x\bar{q}(x) \\ &= A x^a (1-x)^b + C (c+1) (1-x)^c \end{aligned} \tag{10}$$

$$\begin{aligned} x\tilde{F}_3(x) &= xq(x) - x\bar{q}(x) \\ &= A x^a (1-x)^b \end{aligned}$$

such that $x\tilde{F}_3(x)$ represents the valence quark distribution and $\tilde{F}_2(x)$

represents the sum of valence and sea distributions. The parameter C , the integral over the sea-quark content of the nucleon, is used to calculate the relative antiquark content $\bar{q}/(q+\bar{q})$. The CC structure functions of Equation (3) differ from the F by the strange and charm sea contributions. The NC structure functions of Equation (6) differ also by the coupling constants. In the fits to follow we will neglect the charm sea and assume that the contribution of the strange sea is equal to 20% of the total sea.

The ratio $R(x)$ depends upon the NC and CC parameterizations and the NC couplings. We will assume values for the CC parameters consistent with the world's data, and then determine the NC parameters. The resultant NC parameters should then be examined in comparison to the assumed CC parameters. Corrections for event misidentification, cuts, resolutions, and backgrounds are made within the fit procedure.

To determine the NC couplings, and hence $\sin^2\theta_w$, several assumptions are made. In the context of the standard model the NC parameters are assumed to be the same as the CC parameters. The structure functions given in Equations (3) and (6) then differ only by the coupling constants plus terms proportional to the strange and charm sea. The coupling constants are simple functions of $\sin^2\theta_w$. A fit to the ratio $R(x)$ yields the preliminary result

$$\sin^2\theta_w = .243 \pm .014$$

where the error presented is statistical only. The systematic error is currently estimated to be equivalent to the statistical error. No radiative corrections have been made, but are expected to be small. For the remainder of the fits we will assume that the couplings are to be given by the standard model with $\sin^2\theta_w = .24$, and will later examine the sensitivity of our results to this assumption.

In determining the shape parameters of the structure functions, we notice that there is a strong correlation among several of the parameters of Equation (10) when fitting the ratio $R(x)$. We will not attempt to fit all parameters simultaneously, but will instead hold certain parameters fixed and solve for the others. If we assume $c_{NC} = c_{CC} = 7$ and require the Gross - Llewellyn Smith sum rule constraint

$$\int \tilde{F}_3(x) dx = 3$$

we find

	CC	NC
a	.5	.53±.10
b	3.	3.17±.58
$\bar{q}/(q+\bar{q})$.136	.13±.02

If we assume $a_{NC}=a_{CC}=.5$ and $c_{NC}=c_{CC}=7$ we find

	CC	NC
A	3.28	3.33±.58
b	3.	3.02±.34
$\bar{q}/(q+\bar{q})$.136	.14±.02

If we assume $A_{NC}=A_{CC}=3.28$, $a_{NC}=a_{CC}=.5$, $b_{NC}=b_{CC}=3$, $c_{NC}=c_{CC}=7$, and solve for only the relative antiquark content we find

	CC	NC
$\bar{q}/(q+\bar{q})$.136	.14±.01

We conclude that the quark momentum fraction distributions as probed by the NC interaction are consistent with those as determined by the CC interaction.

The analysis of the ratio $R(x)$ reduces the effect of systematic errors. We find the above parameterization fits to be unchanged by systematic changes of up to 10% in the neutrino energy, 10% in the hadron energy, 10% in the hadron angle, or variations in $\sin^2\theta_W$ between 0.22 and 0.25. We also find that an increase in the hadron angular resolution of up to 20% would not alter fit parameters, but would increase fit errors by a similar 20%.

The analysis of the Fermilab - MIT - MSU data demonstrates that an event-by-event measurement of the NC x-distribution is possible in a large fine-grained electronic detector. Restrictive cuts and a selected kinematic regime enhance event identification and reconstruction, and minimize background corrections. The analysis of the ratio $R(x)$ allows comparison of NC to CC with reduced sensitivity to systematic effects.

6. Conclusions

The use of the charged current neutrino interaction as a probe of nucleon structure is well established. Four experiments with differing detectors and analysis techniques have presented results on the study of the nucleon structure using the neutral current neutrino interaction. The bubble chamber experiments have demonstrated the qualitative agreement of the nucleon x-distributions as probed by the NC and the CC interactions, but are hindered from making quantitative statements because of the limitations of small event samples and substantial corrections. The electronic detector experiments, with substantially larger event samples, have taken different approaches to the structure function analysis. The CHARM collaboration analysis relies on an unfolding technique to extract the NC structure functions. Corrections for event classification, neutrino parentage,

and backgrounds are made in the unfolding process. The Fermilab - MIT - MSU collaboration makes an event-by-event measurement of the NC x-distribution, making cuts which enhance event identification and minimize backgrounds. The ratio of the NC x-distribution to the CC x-distribution is examined to minimize sensitivity to systematic error. In fits to the structure functions, both experiments observe no significant difference in the nucleon structure as probed by the weak neutral current or the weak charged current. The expectations of the standard model are confirmed.

REFERENCES

- [1] C.Baltay et al., Phys. Rev. Letters 44 (1980) 916.
- [2] M.Jonker et al., Phys. Lett. 128B (1983) 117.
- [3] C.Baltay et al., Phys. Rev. Letters 52 (1984) 1948.
- [4] D.Bogert et al., IEEE Trans. Nucl. Sci. 29 (1982) 363.

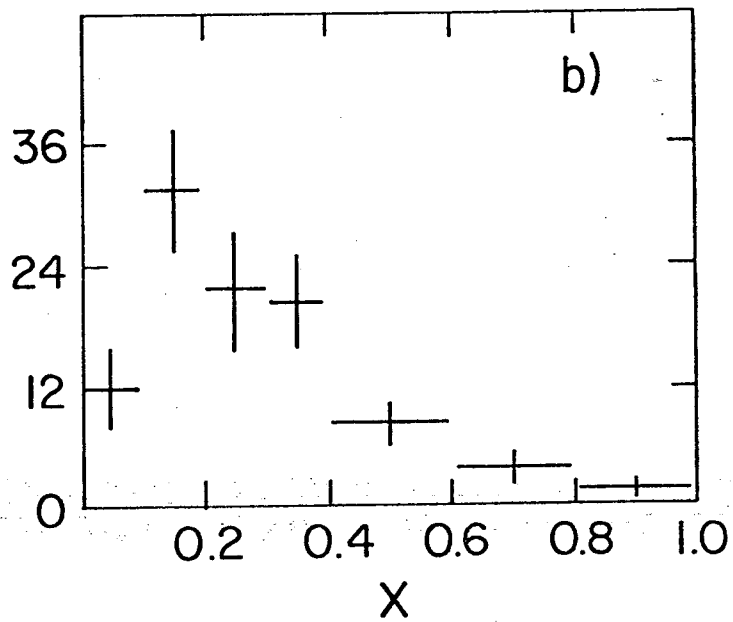
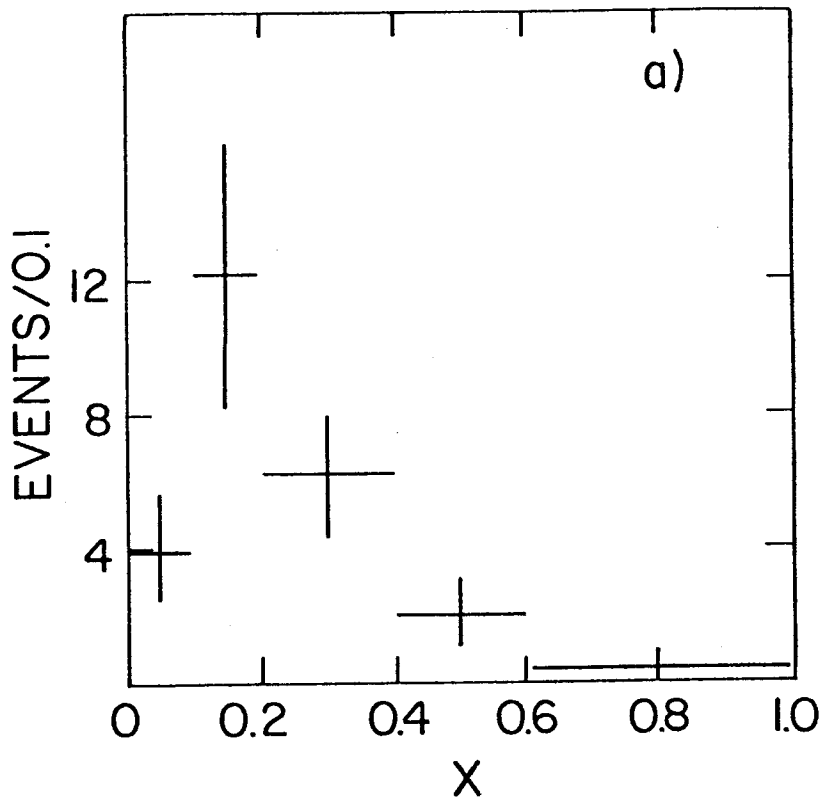


Fig. 1. x-Distributions for (a) NC events, (b) CC events. (Columbia-Rutgers-Stevens)

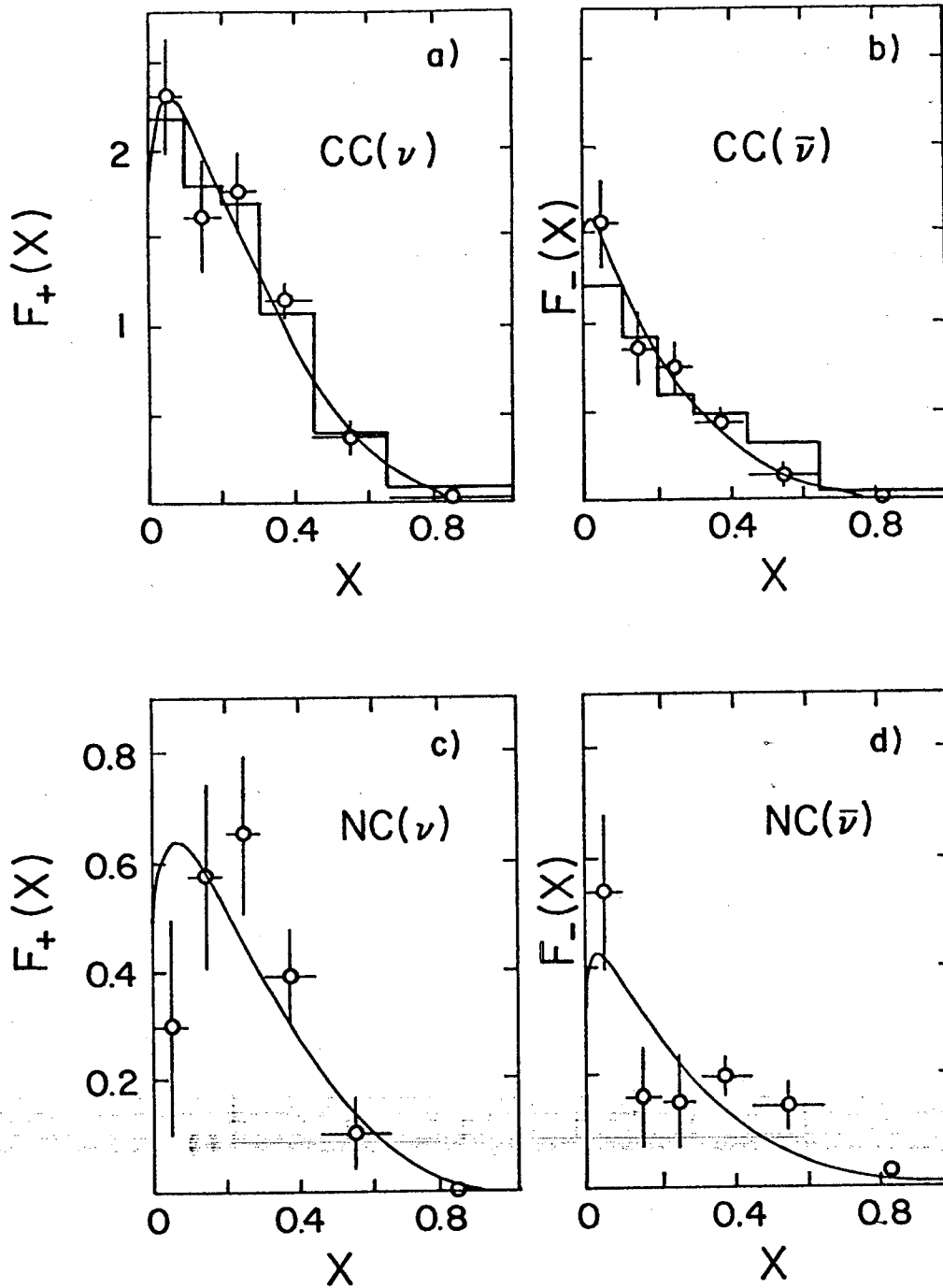


Fig. 2. Structure functions $F_{\pm}(x)$ for (a) $CC \nu$ events, (b) $CC \bar{\nu}$ events, (c) $NC \nu$ events, (d) $NC \bar{\nu}$ events. See text for a description of the fits. (CHARM)

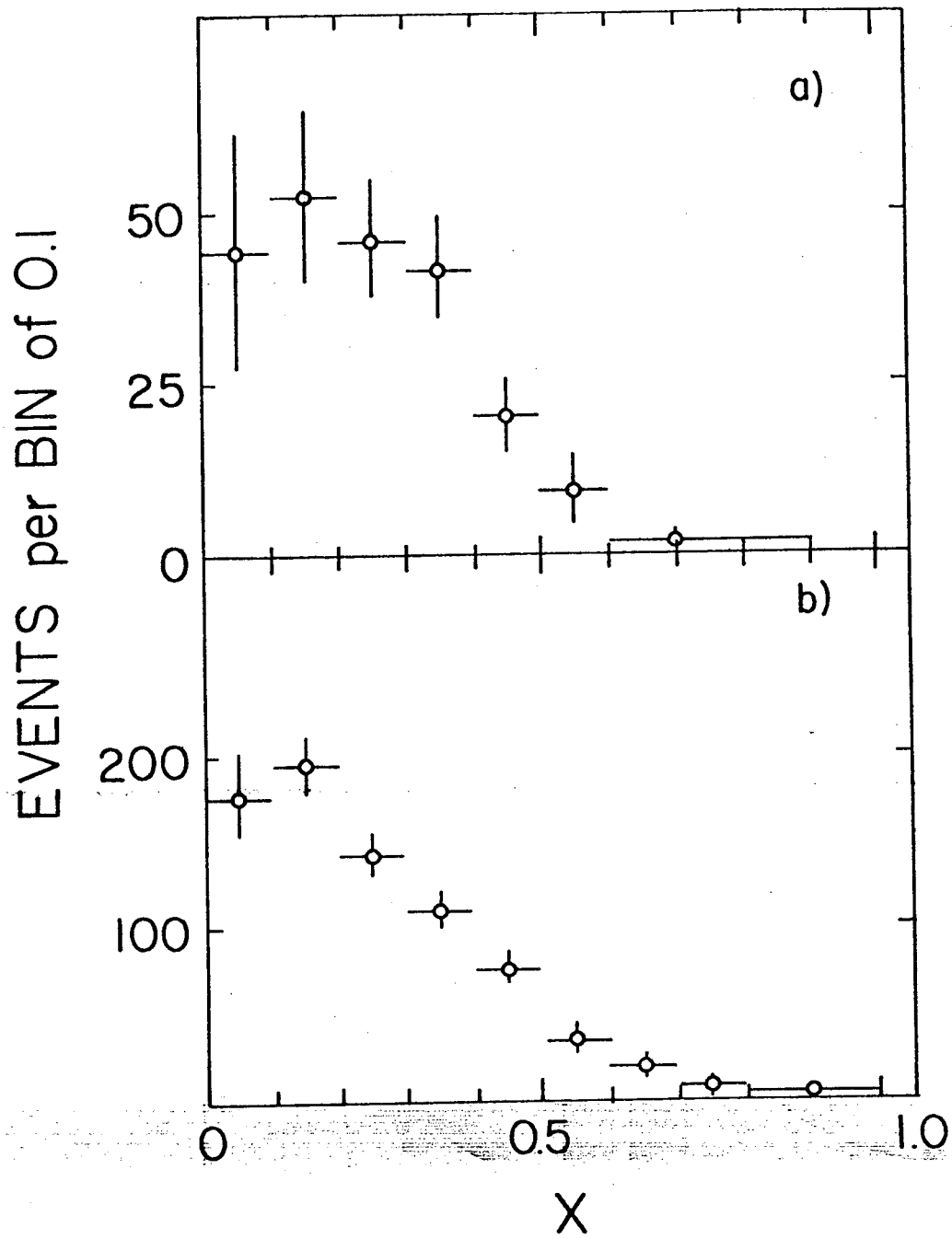


Fig. 3. x -Distribution for (a) NC events, (b) CC events. (Columbia-Rutgers-BNL)

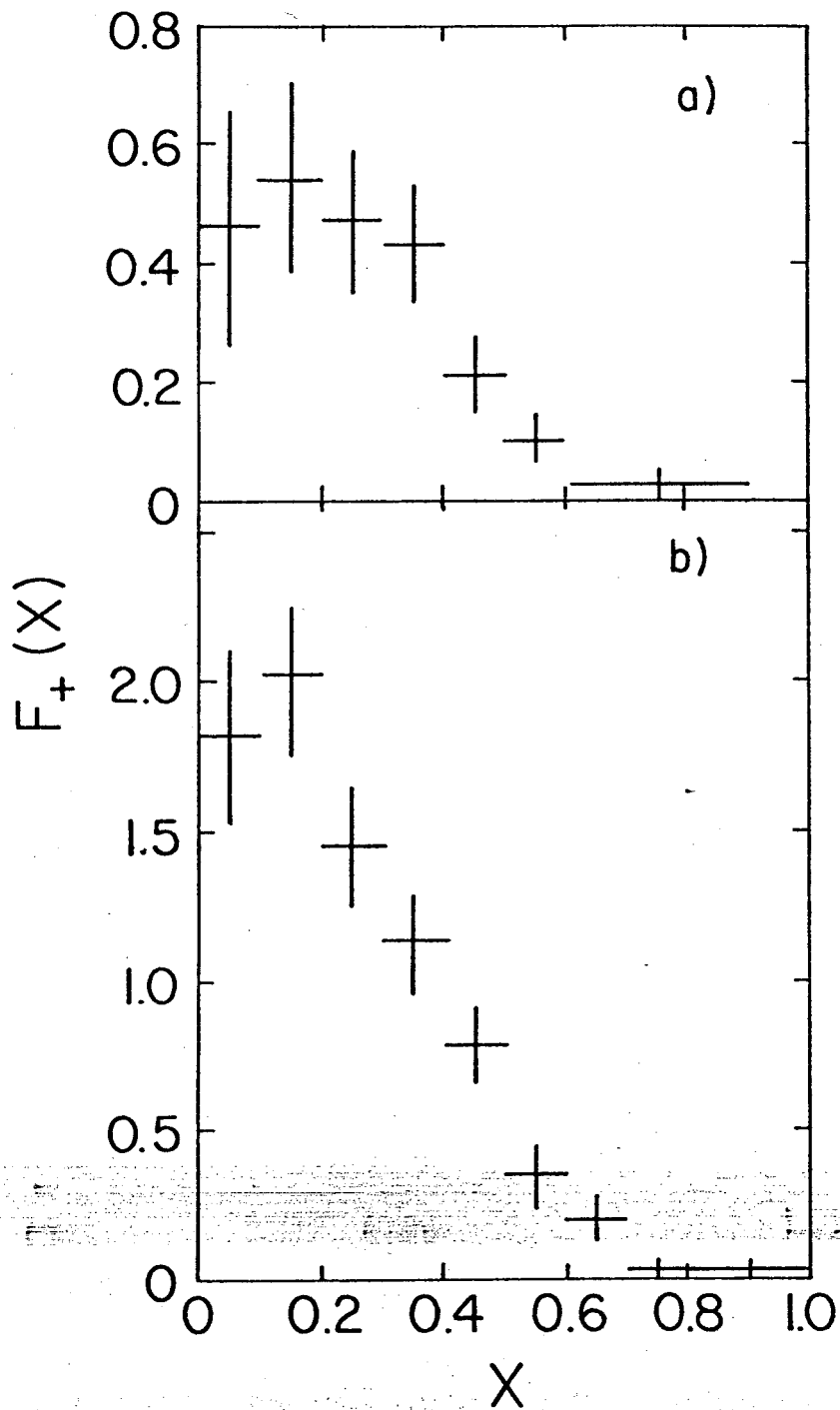


Fig. 4. Structure functions $F_+(x)$ for (a) NC, (b) CC. (Columbia-Rutgers-BNL)

RUN 4724 EVENT 260
HITTOT= 4077
PHT: MAX= 8192 SUM= 28728 HBT= 27629

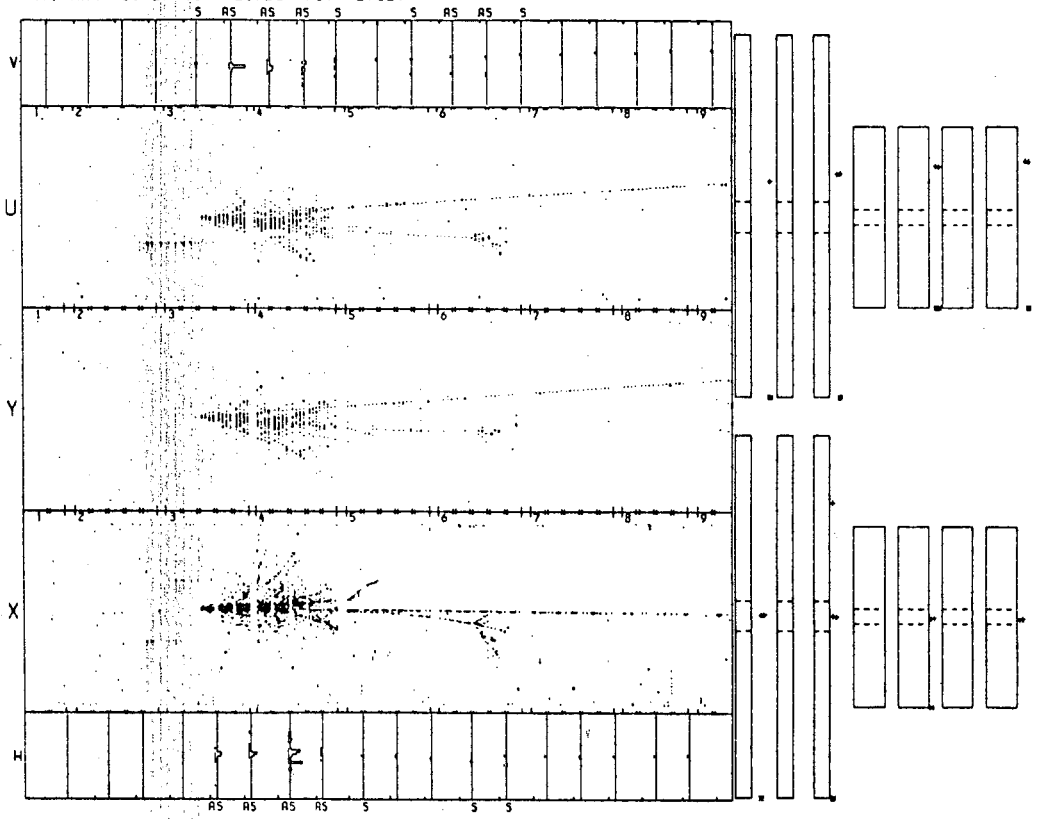


Fig. 5. CC event in the Fermilab-MIT-MSU detector.

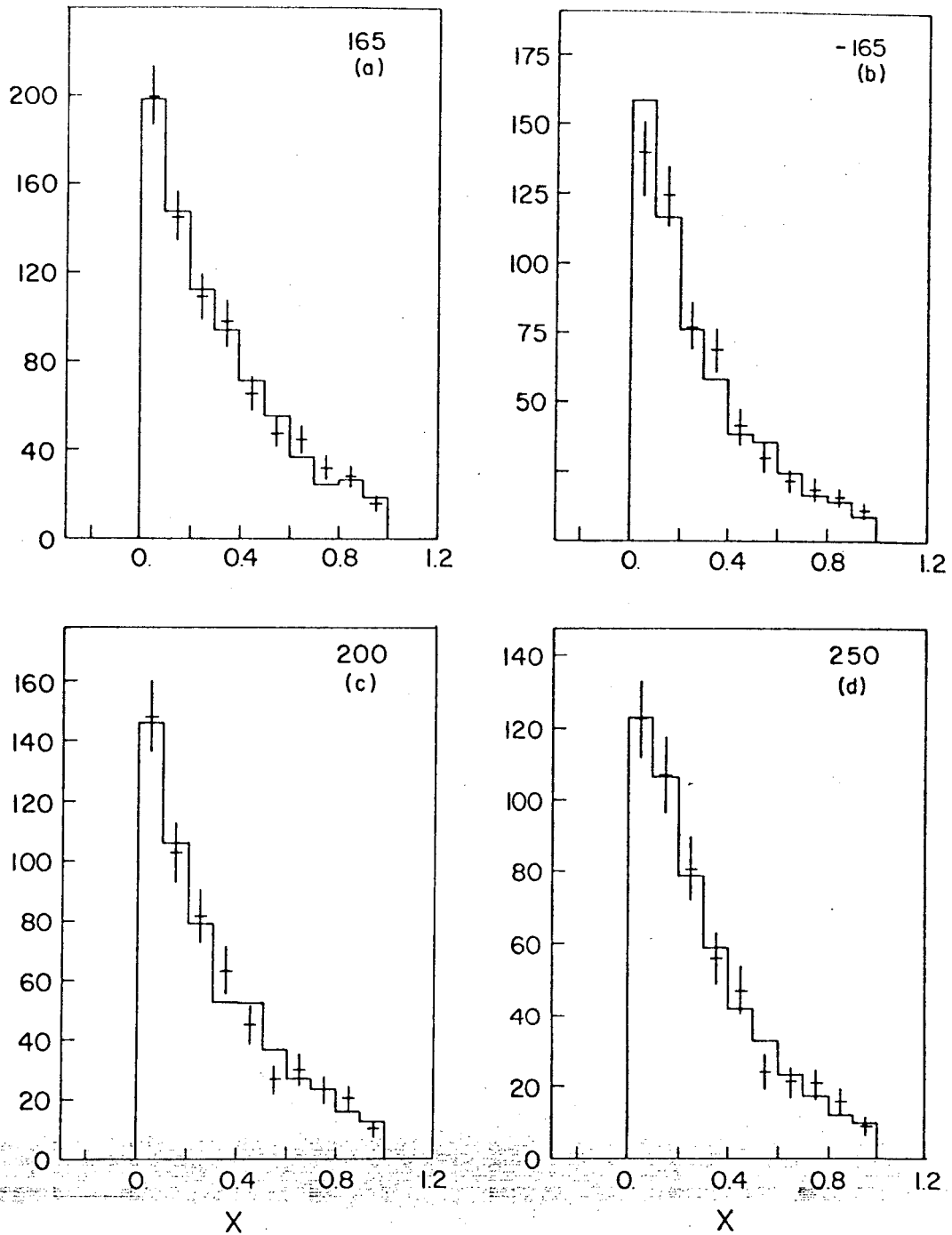


Fig. 6. Measured x-distributions for (a) +165, (b) -165, (c) +200, (d) +250 secondary momentum. Data points are for NC events, histograms are for CC events normalized to equal number of events. (Fermilab-MIT-MSU)

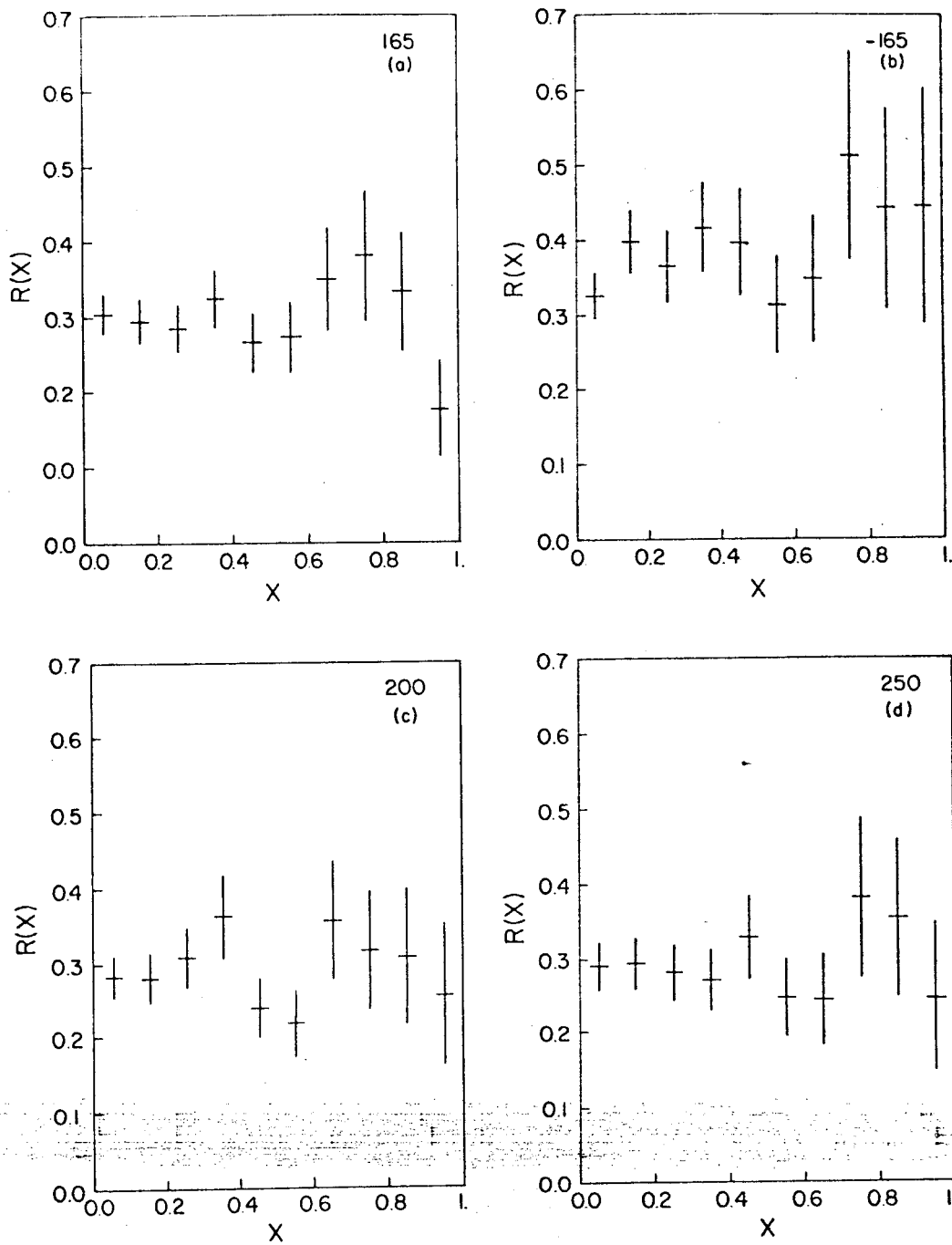


Fig. 7. NC/CC ratio as function of x for (a) +165, (b) -165, (c) +200, (d) +250 secondary momentum. (Fermilab-MIT-MSU)